Alternative Theories of Dark Matter in the Light of Gravitational Lensing

Aysu Ece Saricaoglu

Washington University in St. Louis
Physics Department
a.saricaoglu@wustl.edu

May 9, 2025

2025-05-09

Alternative Theories of Dark Matter in the Light of Gravitational Lensing

Aysu Ece Saricaoglu

Washington University in St. Louis
Physics Department
a.saricaoglu@wustl.edu

May 9, 2025

Hi everyone! Today I'm gonna talk about my research work briefly.

Contents

1 Star-Bound Primordial Black Holes as a Probe of Dark Matter
- Theory
- Preliminary Results
- Future Work

2 Galaxy-Scale Strong Lenses as a Probe of Dark Matter
- Theory
- Preliminary Results
- Future Work

What is Dark Matter, and where to find them?

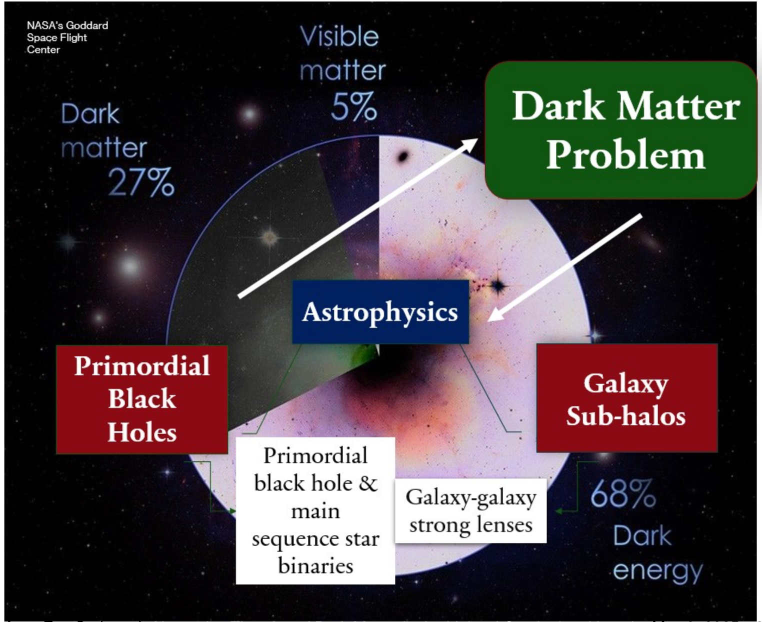

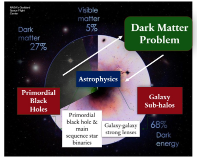

I work on the dark matter problem. I approach this problem from two directions, primordial black holes and galaxy sub-halos. For primordial black holes, I investigate main sequence star – black hole binaries. For sub-halos, I turn to galaxy-galaxy scale strong lenses.

Part I: Star-Bound Primordial Black Holes as a Probe of Dark Matter

Part I: Star-Bound Primordial Black Holes as a Probe of Dark Matter

Our current cosmological model (LambdaCDM) suggests a higher matter density compared to baryon density, so it implies non-baryonic matter in the universe, which we refer to as the dark matter. One of the candidates is the Primordial Black holes

What are primordial black holes?

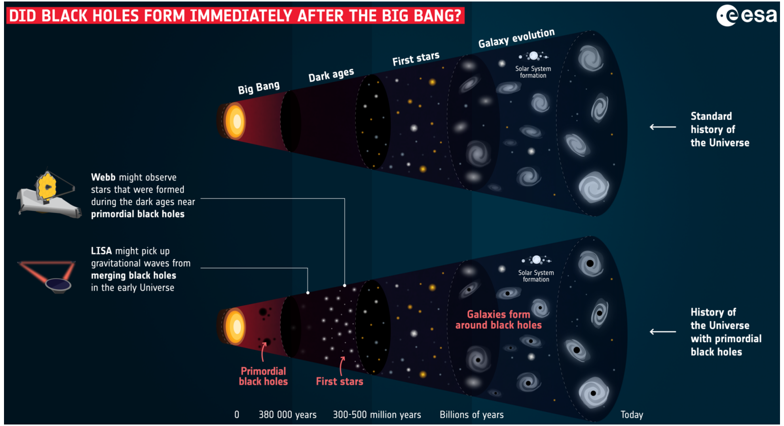

Image credits: European Space Agency (ESA)

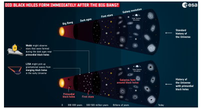

- Primordial black holes are hypothetical objects that could have formed in the early universe, as highly over-dense regions gravitationally collapse.
- They are made of non-baryonic matter and unlike black holes we know of so far, they have non-stellar origins.

PBHs as Cold Dark Matter Candidates

- Unless the limits from evaporation and CMB limits from Planck are relaxed the scenario of the dark matter fully composed of PBH is ruled out [11].
- The effect of various PBH fractions on the total power spectrum of the DM density field is shown in figure below compared to standard ΛCDM model [27].

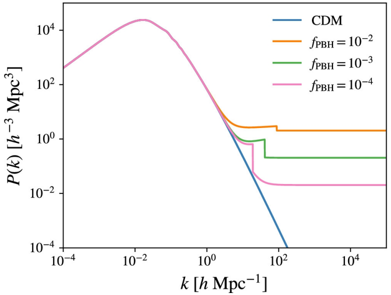

Adapted from Zhang, Bromm, and Liu [27] (Figure 1).

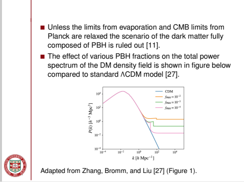
Unless the limits from evaporation and CMB limits from Planck are relaxed the scenario of the dark matter fully composed of PBH is ruled out [11].
The effect of various PBH fractions on the total power spectrum of the DM density field is shown in figure below compared to standard ΛCDM model [27].
Adapted from Zhang, Bromm, and Liu [27] (Figure 1).

PBHs can provide a compelling explanation for the dark matter problem. In figure mPBH = 33 Msun, they choose this mass because it is the location of the (secondary) Gaussian peak in the best-fit Power-Law + Peak model of the mass distribution of BHs detected in GW observations of binary BH mergers by the LIGO-Virgo-KAGRA Scientific Collaboration. Varying mPBH by a factor of a few does not change our conclusions

Why Black Hole - Main Sequence Star (BH-MS) Binaries?

- Primordial black holes in binary systems are detectable by their impact on the binary star light curves as a result of self-lensing.
- Initial work on compact object (CO) self-microlensing detectability considered MS star companions as unfavorable candidates compared to white dwarfs, since the source radius and the lens effect are inversely proportional [1].
- However, having more achievable photometry on brighter targets and a higher population to be monitored, Rahvar et al. [19] showed that MS stars are not less favorable targets than other CO.

- Primordial black holes in binary systems are detectable by their impact on the binary star light curves as a result of self-lensing.
- Initial work on compact object (CO) self-microlensing detectability considered MS star companions as unfavorable candidates compared to white dwarfs, since the source radius and the lens effect are inversely proportional [1].
- However, having more achievable photometry on brighter targets and a higher population to be monitored, Rahvar et al. [19] showed that MS stars are not less favorable targets than other CO.

- Primordial black holes in binary systems are detectable by their impact on the binary star light curves as a result of self-lensing.
- Self-lensing in binary systems occurs when the compact object gravitationally deflects the light from the star as it transits.

Possible Scenarios for BH-MS Formation

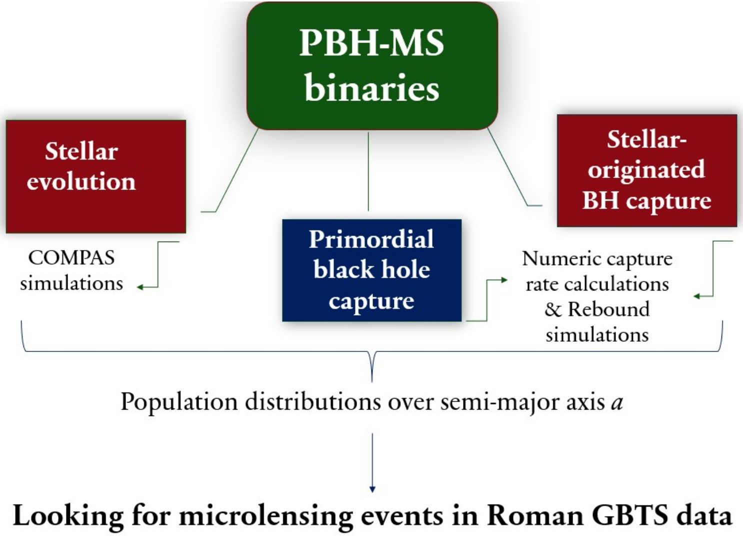

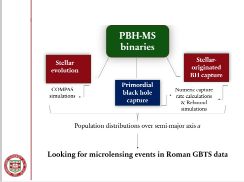

$\Rightarrow$ Besides the scenario in which the dark matter-originated PBH is captured by a star, any BH-MS binary we observe is a possible candidate for two additional scenarios.

- i. Formation by stellar evolution process
- ii. Formation by stellar-originated black hole capture

Possible Scenarios for BH-MS Formation

⇒ We need to be able to distinguish the scenarios of stellar binary evolution, dynamical capture of a stellar-originated BH, and capture of a PBH.
↪ In most cases, there is a degeneracy in the mass dimension of such systems.
⇒ However, the degeneracy on the semimajor axis for these three subpopulations of the BH-MS binaries might break.

> I propose to use semimajor axis distributions to resolve the origins of the binary systems that will be detected by microlensing events.

⇒ We need to be able to distinguish the scenarios of stellar binary evolution, dynamical capture of a stellar-originated BH, and capture of a PBH.
↪ In most cases, there is a degeneracy in the mass dimension of such systems.
⇒ However, the degeneracy on the semimajor axis for these three subpopulations of the BH-MS binaries might break.
I propose to use semimajor axis distributions to resolve the origins of the binary systems that will be detected by microlensing events.

- So let's assume we observed such a binary system, we need to be able to distinguish these three scenarios to tell if the black hole in the binary is a PBH or not
- To do that, we may look at the distributions over semimajor axis for each population. If they have occurrence rates that peak at distinct semimajor axis values we might have a clue about their origins.

Stellar Evolution Binary System Distributions

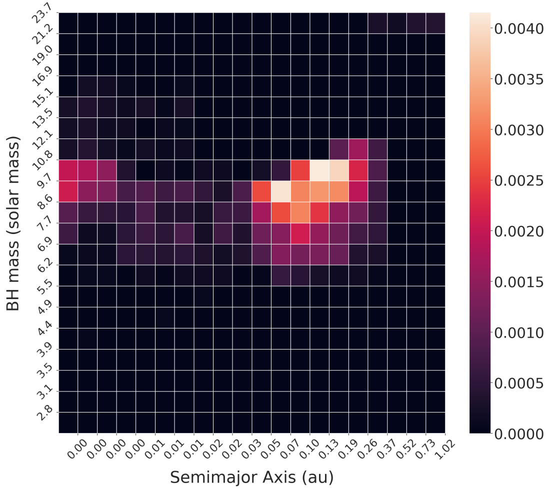

Occurence rate distribution over primary mass and semimajor axis for BH-MS binaries after their last MT event for $T < 70$ (days).

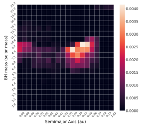

- I use the stellar binary population synthesis tool COMPAS to simulate parameter distribution of the systems formed by evolution.
- Here, you see the distribution of MS-PBH binary systems after their last mass transfer event over their separation distance.

We take the mean occurrence plots on Masuda & Hotokezaka's work [14] as a basis to compare with our simulation results.

Prospects of Finding Detached Black Hole–Star Binaries with *TESS*

Kento Masuda[1] and Kenta Hotokezaka
Department of Astrophysical Sciences, Princeton University, Princeton, NJ 08544, USA; kmasuda@astro.princeton.edu
Received 2018 August 31; revised 2019 August 1; accepted 2019 August 8; published 2019 October 1

Abstract

We discuss prospects of identifying and characterizing black hole (BH) companions to normal stars on tight but detached orbits, using photometric data from the *Transiting Exoplanet Survey Satellite* (*TESS*). We focus on the following two periodic signals from the visible stellar component: (i) in-eclipse brightening of the star due to gravitational microlensing by the BH (self-lensing), and (ii) a combination of ellipsoidal variations due to tidal distortion of the star and relativistic beaming due to its orbital motion (phase-curve variation). We evaluate the detectability of each signal in the light curves of stars in the *TESS* input catalog, based on a pre-launch noise model of *TESS* photometry as well as the actual light curves of spotted stars from the prime *Kepler* mission to gauge the potential impact of stellar activity arising from the tidally spun-up stellar components. We estimate that the self-lensing and phase-curve signals from BH companions, if they exist, will be detectable in the light curves of effectively $\mathcal{O}(10^5)$ and $\mathcal{O}(10^6)$ low-mass stars, respectively, taking into account orbital inclination dependence of the signals. These numbers could be large enough to actually detect signals from BHs: simple population models predict some 10 and 100 detectable BHs among these "searchable" stars; although, the latter may be associated with a comparable number of false positives due to stellar variabilities, and additional vetting with radial velocity measurements would be essential. Thus, the *TESS* data could serve as a resource to study nearby BHs with stellar companions on shorter-period orbits than will potentially be probed with *Gaia*.

Key words: stars: black holes – stars: neutron – techniques: photometric – white dwarfs

We take the mean occurrence plots on Masuda & Hotokezaka's work [14] as a basis to compare with our simulation results.

Residuals

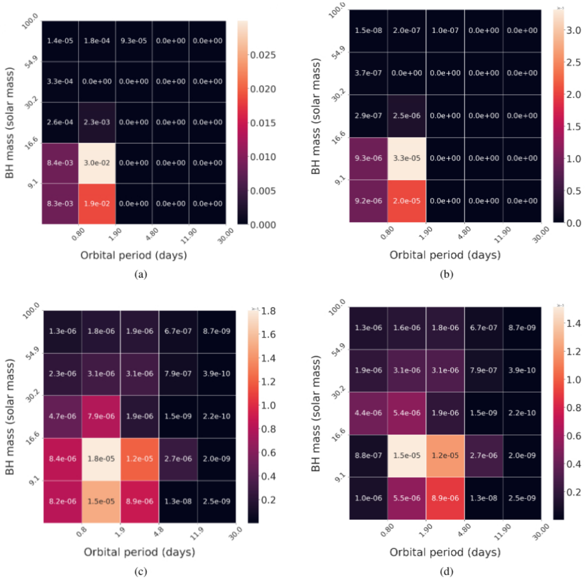

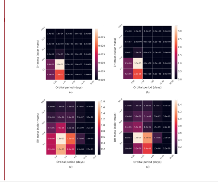

(a) Occurrence rate distribution over black hole mass and orbital period for BH-MS binaries after their last MT event for $T < 30$ (days), (b) after applying searchability index of 0.0011, (c) occurrence rate distribution over black hole mass - orbital period for binaries searchable via self lensing adapted Figure 4b by Masuda and Hotokezaka [14], (d) residuals of b & c. Stellar evolution simulation by COMPAS processed by LUXETENEBRAE.

Residuals

⇒In Masuda & Hotokezaka [15], the 'searchability' constraint includes various criteria such as recovery rate as a function of the signal-to-noise ratio C_{rec} and the eclipse probability R_{star}/a

$$N_{eff} = \frac{R_{star}}{a} C_{rec}(\sqrt{n}\frac{S_{self-lensing}}{\sigma_{30min}}) \tag{1}$$

while the values compared above only include the criteria of edge-on configuration for the binaries, given by $cos_i \leq cos(89.9) \approx cos(\pi/2) = 0$

$$cos_i \leq cos(89.9) \approx cos(\pi/2) = 0 \tag{2}$$

which yields a *searchability index* of ≈ 0.0011.

⇒In Masuda & Hotokezaka [15], the 'searchability' constraint includes various criteria such as recovery rate as a function of the signal-to-noise ratio C_{rec} and the eclipse probability R_{star}/a

$$N_{eff} = \frac{R_{star}}{a} C_{rec}(\sqrt{n}\frac{S_{self-lensing}}{\sigma_{30min}}) \tag{1}$$

while the values compared above only include the criteria of edge-on configuration for the binaries, given by $cos_i \leq cos(89.9) \approx cos(\pi/2) = 0$

$$cos_i \leq cos(89.9) \approx cos(\pi/2) = 0 \tag{2}$$

which yields a *searchability index* of ≈ 0.0011.

The main cause of the current residual values is the duality of the searchability criteria. I will evaluate the additional constraints and minimize the residuals to confirm that the occurrence rates from COMPAS simulation are reasonable and in line with the occurrence rates expected from TESS by Masuda and Hotokezaka [14]. Then, in the first part of this task, I will search for microlensing events in TESS data with predicted mass and semimajor axis parameters to compare with the COMPAS results. A discrepancy between the predicted and observed populations where observed abundancy is higher or a discrepancy of the peak semimajor axis might indicate BH-MS systems formed by capture.

Among three mechanisms for the dynamical capture explained in detail by Lehmann et al. [12], in this work, I focus on two cases:

1. Losing energy to gravitational radiation due to rapid acceleration during single-body encounters, and becoming bound to the same object.
2. Losing mechanical energy to one object and becoming bound to another during a few-body encounter.

Among three mechanisms for the dynamical capture explained in detail by Lehmann et al. [12], in this work, I focus on two cases:

1. Losing energy to gravitational radiation due to rapid acceleration during single-body encounters, and becoming bound to the same object.
2. Losing mechanical energy to one object and becoming bound to another during a few-body encounter.

Capture cross section from gravitational radiation

Power radiated is given by the quadruple formula [7]

$$P = -\frac{G}{5c^2}\left\langle \frac{d^3 J_{ij}}{dt^3}\frac{d^3 J^{ij}}{dt^3}\right\rangle \tag{3}$$

$\rightarrow J_{ij}$:reduced quad. moment $\Rightarrow J_{ij} = I_{ij} - \frac{1}{3}\delta_{ij}\delta^{kl} I_{kl}$
$\rightarrow I_{ij}$:quad. moment tensor $\Rightarrow I(t)_{ij} = \int y^i y^j T^{00}(t,y) d^3 y$

$$\Delta E_{GW} = \int_{-\infty}^{\infty} P(t)dt = \frac{8}{15}\frac{G^{7/2}}{c^5}\frac{M^{1/2} m_1^2 m_2^2}{r_{min}^{7/2}} g(e) \tag{4}$$

$$g(e) = \frac{\left[24\cos^{-1}\left(-\frac{1}{e}\right)\left(1+\frac{73}{24}e^2+\frac{37}{96}e^4\right)+\left(e^2-1\right)^{1/2}\left(\frac{301}{6}+\frac{673}{12}e^2\right)\right]}{(1+e)^{7/2}}$$

Power radiated is given by the quadruple formula [7]
$$P = -\frac{G}{5c^2}\left\langle \frac{d^3 J_{ij}}{dt^3}\frac{d^3 J^{ij}}{dt^3}\right\rangle \tag{3}$$
$\rightarrow J_{ij}$:reduced quad. moment $\Rightarrow J_{ij} = I_{ij} - \frac{1}{3}\delta_{ij}\delta^{kl} I_{kl}$
$\rightarrow I_{ij}$:quad. moment tensor $\Rightarrow I(t)_{ij} = \int y^i y^j T^{00}(t,y) d^3 y$
$$\Delta E_{GW} = \int_{-\infty}^{\infty} P(t)dt = \frac{8}{15}\frac{G^{7/2}}{c^5}\frac{M^{1/2} m_1^2 m_2^2}{r_{min}^{7/2}} g(e) \tag{4}$$
$$g(e) = \frac{\left[24\cos^{-1}\left(-\frac{1}{e}\right)\left(1+\frac{73}{24}e^2+\frac{37}{96}e^4\right)+\left(e^2-1\right)^{1/2}\left(\frac{301}{6}+\frac{673}{12}e^2\right)\right]}{(1+e)^{7/2}}$$

From here, we turn to binaries formed by capture. First capture mechanism we will investigate is the capture by energy loss due to gravitational wave emission.GW solutions come from the linearized field equations where space-time is considered to have the Minkowski metric, and Einstein's equation coupled to matter, where the strain tensor represents the gravitational waves [7].
In this solution, the power radiated is given by the quadruple formula. ($I(t)_{ij}$ depends on the trajectories of the bodies in the encounter system.Then, the gravitational energy loss can be computed by [23] where *enhancement factor*:$g(e)$ for $e \geq 1$

Capture cross section from gravitational radiation

$$r_{min} = \frac{GM}{v_\infty^2}(e-1) = \frac{GM_S}{v_\infty^2}\left(\sqrt{1+\frac{b^2 v_\infty^4}{G^2 M_S^2}}-1\right) \quad (5)$$

Setting $r_{min} = R_S$ for R_S:radius of the star

$$b_{min} = \sqrt{R_S^2 + \frac{2GM_S R_S}{v_\infty^2}} \quad (6)$$

$b_{max} \rightarrow$ solved numerically.
$\Rightarrow$Capture condition:

$$\Delta E_{GW} > \frac{1}{2} M_{PBH} v_\infty^2$$

To avoid collisions, we set $r_{min} = R_S$ where R_S is the radius of the star, [12]. b_{max} requires numerical calculations. We start by imposing the capture condition $\Delta E_{GW} > \frac{1}{2} M_{PBH} v_\infty^2$ that indicates the energy loss due to GW is enough to turn PBH's energy negative so that the encounter yields an elliptic trajectory ($e < 1$) in which PBH becomes bound to the star. For $e < 1$, the encounter is a hyperbolic trajectory, PBH remains unbound with positive energy, and escapes after the event. $e = 1$ gives a parabolic trajectory with zero energy, and $e < 1$ results in an elliptic trajectory with negative energy, PBH becomes bound to the star.

Capture cross section from gravitational radiation

Capture crossection by gravitational wave emission σ_{cap}^{GW} [12]

$$\sigma_{cap}^{GW} = \pi(b_{max} - b_{min})^2 \Theta(b_{max} - b_{min}) \tag{7}$$

hence the capture rate

$$R_{cap}^{GW} = n_\infty \langle \sigma_{cap} v_\infty \rangle = n_\infty \int dv f_\infty(v) \sigma_{cap} v \tag{8}$$

where

$$f_\infty(v) \propto v^2 exp(-\frac{v^2}{v_0^2}) \Theta(v_{esc} - v) \tag{9}$$

we take $v_0 = 220$km/s & $v_{esc} = 550$km/s

Capture crossection by gravitational wave emission σ_{cap}^{GW} [12]
$\sigma_{cap}^{GW} = \pi(b_{max} - b_{min})^2 \Theta(b_{max} - b_{min})$ (7)
hence the capture rate
$R_{cap}^{GW} = n_\infty \langle \sigma_{cap} v_\infty \rangle = n_\infty \int dv f_\infty(v) \sigma_{cap} v$ (8)
where
$f_\infty(v) \propto v^2 exp(-\frac{v^2}{v_0^2}) \Theta(v_{esc} - v)$ (9)
we take $v_0 = 220$km/s & $v_{esc} = 550$km/s

n_∞ is the number density of objects far from the system and angle brackets denote the average over velocities.
f(v) This probability density is an approximate description of the equilibrium distribution of DM particles — in our case, PBHs — throughout the halo. Near a point mass like a star, the velocity distribution is modified by the local gravitational potential. Thus, f(v) should be treated as the distribution of particles far from the stellar system.

Capture cross section from gravitational radiation

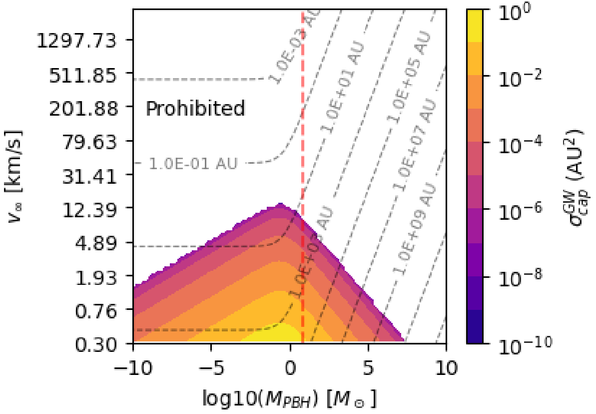

σ^{GW}_{cap} for GRO J0422 + 32 (V518 Per). Red dashes denote the mass of the black hole used in the calculations, $M_{BH} = 6.5\mathrm{M}_\odot$. Grey dashes show the semi-major axis values right after the capture.

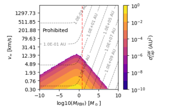

σ^{GW}_{cap} for GRO J0422 + 32 (V518 Per). Red dashes denote the mass of the black hole used in the calculations, $M_{BH} = 6.5\mathrm{M}_\odot$. Grey dashes show the semi-major axis values right after the capture.

Here you can see an example calculation following this procedure. This is the Smallest BH detected so far. Its companion is a main sequence star
The system has a 5h period, which approximately makes T = 5h 4m 35s $\approx a = 0.01326$ AU. We see that GW capture semimajor axis values are much higher than this, it it were formed by capture.

Capture crossection from 3-body encounters

For fixed v_∞,

$$\widetilde{N} = \widetilde{R_{cap}} / \widetilde{R_{ej}} \tag{10}$$

$$\langle \widetilde{N} \rangle = \int \frac{\widetilde{R}_{cap}}{\widetilde{R}_{ej}} = n_\infty \int d\mathbf{v}_\infty \, f(v_\infty) \, \frac{\widetilde{\sigma}_{cap}(v_\infty) v_1(v_\infty)}{\widetilde{R}_{ej}(v_\infty)} \tag{11}$$

where $\widetilde{\sigma}_{cap}$ is integrated over *da* & *de*
Also,

$$\widetilde{R}_{ej} \propto \eta(a, e), \quad \xi(a), \quad \kappa_\pm(\eta, \xi) \tag{12}$$

To obtain a closed-form estimate, we can use mean values instead of integrating over *da* & *de*

$$a :\to \bar{a}, \quad e :\to \bar{e}(\bar{a}) = \frac{1}{2}(1 + e_{min}) \tag{13}$$

We're essentially interested in the expected number of captured PBHs by the star.
If the captured objects do not interact among themselves, then the capture rate is independent of the number of captured objects.
We can thus estimate N for fixed vinf and can average over the population.

Capture crossection from 3-body encounters

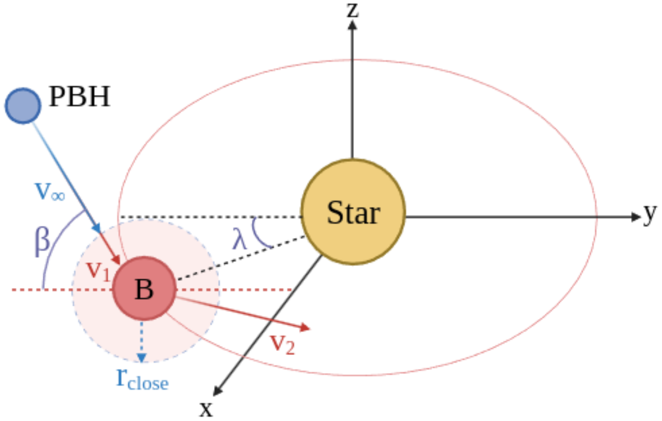

3-body encounter system of the main sequence star, celestial body B, and incident PBH. PBH with velocity v_∞ at infinity, has a close encounter with body B in the shaded region with initial velocity v_1 and exits the encounter with velocity v_2.

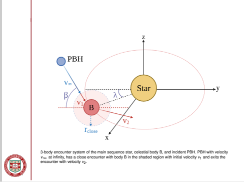

Both capture and ejection crossections depend on several parameters on the encounter geometry. But we need to evaluate abar and bear to go to the rate estimates from the crossections. For that, we simulate encounter events and get distributions for the population.

Case I | Example #1: Stable

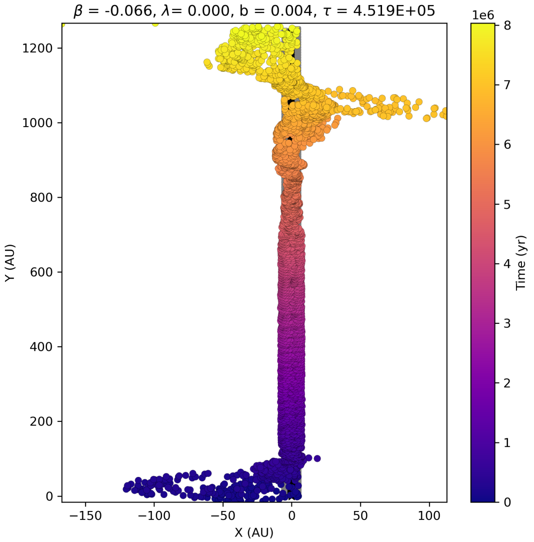

2025-05-09

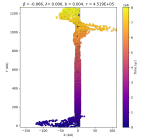

Case I | Example #1: Stable

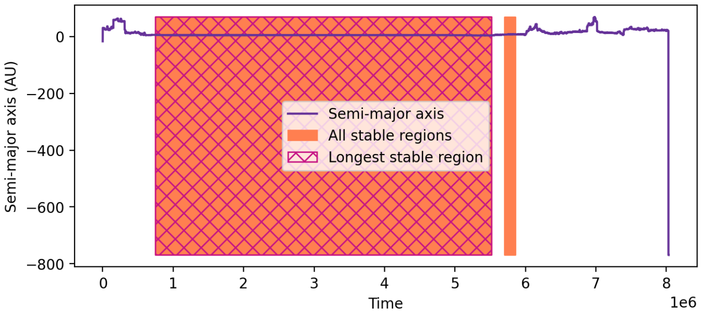

In the paper I am following, for the semimajor axis distributions, they use the value for right after the capture and take the mean. Since observational feasibility is important in my case, I consider the periods where the PBH has stability during its capture lifetime. So instead of taking a single value, I decided to use time averaging over the stable periods

Case I | Example #2: Semi-stable

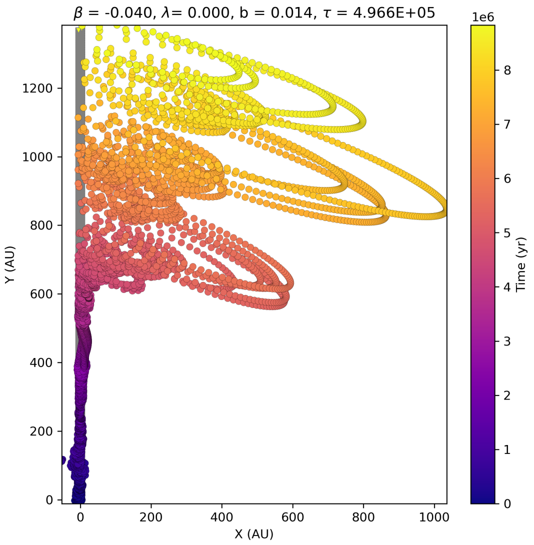

2025-05-09

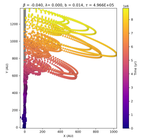

Case I | Example #2: Semi-stable

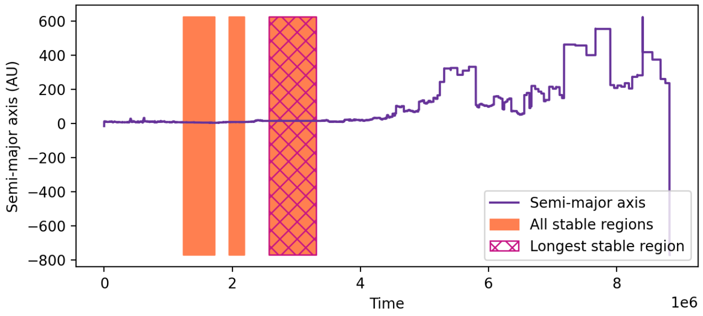

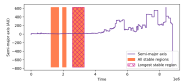

Case I | Example #3: Looks stable?

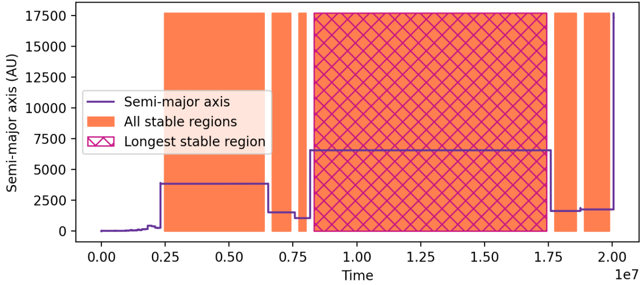

Case I | Example #3: Looks stable?
2025-05-09

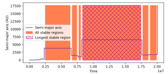

Case I | Example #3: Not so stable...

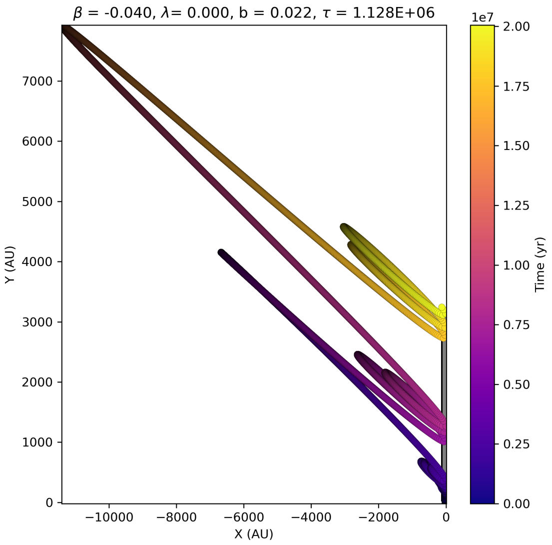

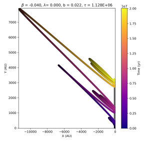

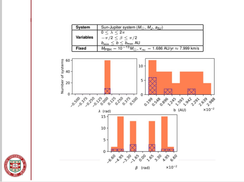

Case I | Initial Parameters

System	Sun-Jupiter system ($M_\odot$, M_J, a_{SJ})
Variables	$0 \leq \lambda \leq 2\pi$ $-\pi/2 \leq \beta \leq \pi/2$ $b_{\text{min}} \leq b \leq b_{\text{max}}$ AU
Fixed	$M_{\text{PBH}} = 10^{-13} M_\odot$, $v_\infty = 1.686$ AU/yr ≈ 7.999 km/s

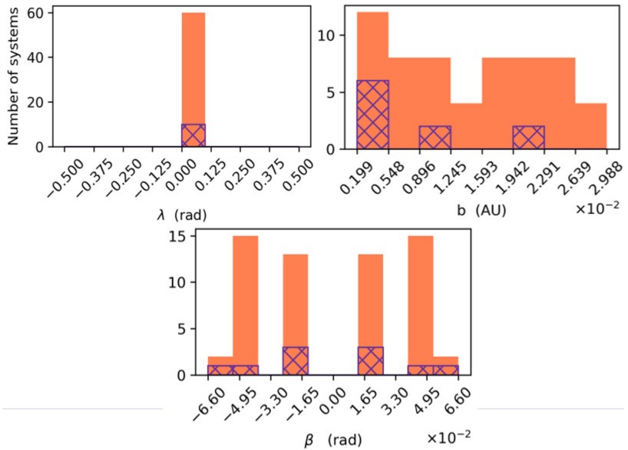

In the first case, we try to find the most optimal encounter direction on beta and lambda, and the distance which is the impact parameter so they are the variables we integrate over on a 3 dimensional grid. All of the masses and the v infinity are fixed.

Case I | Population Yield

Captured Systems	60 sys. with $\tau_{\mathrm{cap}} \geq 10^3\, T_{\mathrm{Jupiter}} \approx 12000$ yr
Stable Orbits	10 sys. with ≥ 1000 yr cont. stability
Stable *a* Stats	$\langle a \rangle = 4.897$ AU, $\langle a \rangle_d = 5.180$ AU

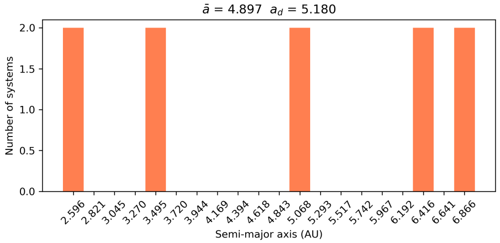

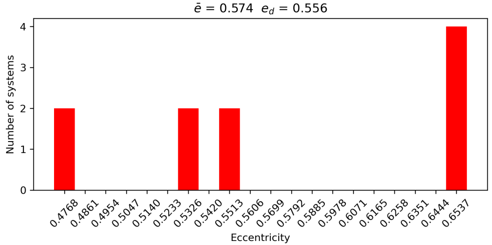

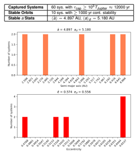

Case II | Initial Parameters

System	Sun-Jupiter system ($M_\odot$, M_J, a_{SJ})
Variables	$10^{-13} \leq M_{\mathrm{PBH}} \leq 10^{-4}$ $1 \leq v_\infty \leq 100$ km/s $b_{\mathrm{min}} \leq b \leq b_{\mathrm{max}}$ AU
Fixed	$\lambda = 0.0$, $\beta = 0.013$ rad

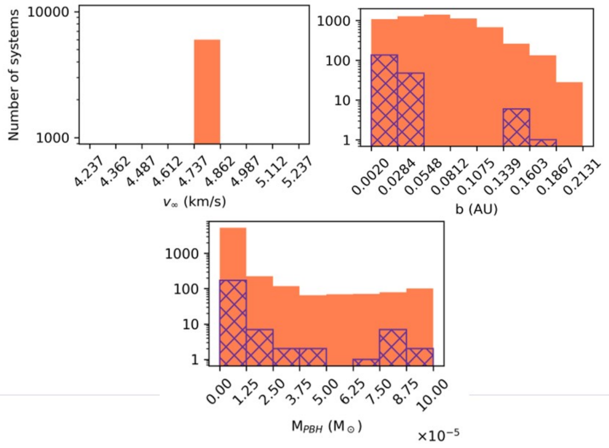

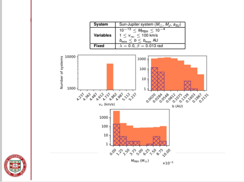

In this case, we fix two angular parameters to the values favored by the first case, and integrate over PBH mass and vinfinity, similar to the GW capture case. Compared to the first case 100 times more systems survive

Case II | Population Yield

Captured Systems	6000 sys. $\tau_{\text{cap}} \geq 10^3\, T_{\text{Jupiter}} \approx 12000$ yr
Stable Orbits	192 sys. with ≥ 1000 yr cont. stability
Stable *a* Stats	$\langle a \rangle = 5.438$ AU, $\langle a \rangle_d = 4.625$ AU

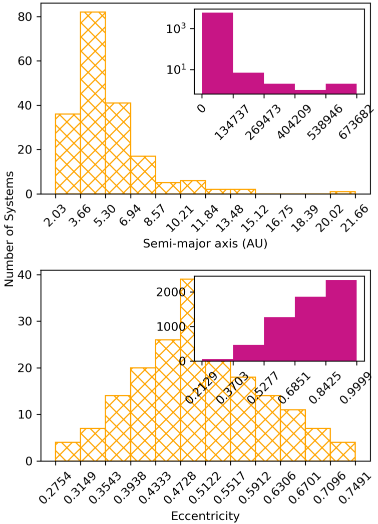

Case III | Initial Parameters

System	Sun-X System ($M_\odot$, M_X, a_{SX})
Variables	$10^{-3} \leq M_X \leq 10^{3.02}$ $M_{Jupiter}$ $1 \leq v_\infty \leq 100$ km/s $0.0046 \leq a \leq 100$ AU
Fixed	$M_{\rm PBH} = 10^{-13} M_\odot$, $\lambda = 0.0$, $\beta = 0.013$ rad, b=$\bar{b}$

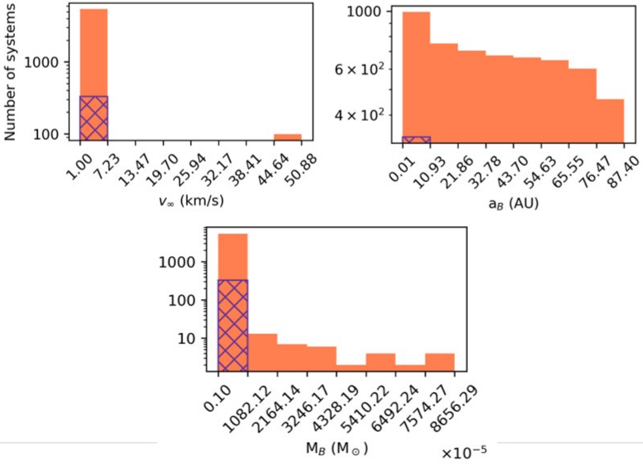

Alternative Theories of Dark Matter in the Light of Gravitational Lensing
Star-Bound Primordial Black Holes as a Probe of Dark Matter
Preliminary Results
Case III | Initial Parameters

2025-05-09

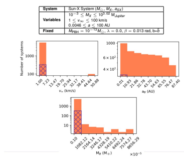

2025-05-09

Case III | Population Yield

Captured Systems	5496 sys. $\tau_{\text{cap}} \geq 10^3\, T_{\text{Jupiter}} \approx 12000$ yr
Stable Orbits	329 sys. with $\geq$ 1000 yr cont. stability
Stable *a* Stats	$\langle a \rangle = 36.299$ AU, $\langle a \rangle_d = 27.112$ AU

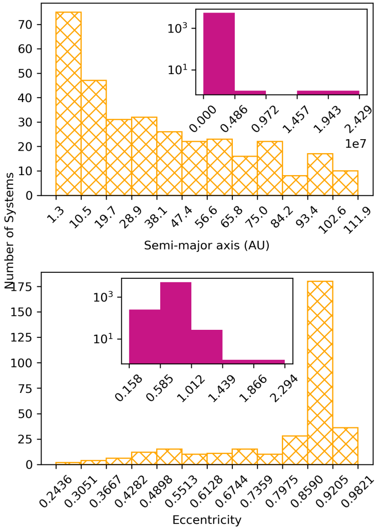

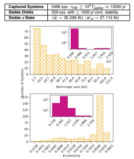

About what we proposed...

From evolution simulation and the capture calculations we roughly see that binaries evolved together undergoing mass transfer events have $a < 1$ AU while those formed by capture have $a > 1$ AU.
For ≤ 120 AU, $a_{\text{min}} = 2.48$ from the first case, $a_{\text{min}} = 1.65$ AU from the second case, for stable durations

From evolution simulation and the capture calculations we roughly see that binaries evolved together undergoing mass transfer events have $a < 1$ AU while those formed by capture have $a > 1$ AU.
For ≤ 120 AU, $a_{\text{min}} = 2.48$ from the first case, $a_{\text{min}} = 1.65$ AU from the second case, for stable durations

From evolution simulation and the capture calculations we roughly see that binaries evolved together undergoing mass transfer events have $a < 1$AU while those formed by capture have $a > 1$ AU.
Considering what we observe so far, the idea of inspecting black hole origins using the distributions over semimajor axis seems to make sense.

Preliminary conclusions

1. v_{inf} of stellar BHs kicked out of their binaries and free floating PBH might be different, directly affecting the capture rates with any methods
2. For now, capture rate calculations from GW can be used to test the possibility of forming by capture of an observed system. In my future work, I will eventually derive the capture rates.

1. v_{inf} of stellar BHs kicked out of their binaries and free floating PBH might be different, directly affecting the capture rates with any methods
2. For now, capture rate calculations from GW can be used to test the possibility of forming by capture of an observed system. In my future work, I will eventually derive the capture rates.

From evolution simulation and the capture calculations we roughly see that binaries evolved together undergoing mass transfer events have $a < 1$AU while those formed by capture have $a > 1$ AU.
Considering what we observe so far, the idea of inspecting black hole origins using the distributions over semimajor axis seems to make sense.

What's Next?

- Evaluation $\langle \bar{N} \rangle$ from the three-body capture and ejection crossections calculated so far
- More simulations on a larger variety of initial parameters, better analysis of the relation between the parameters that enable capture events and their occurrence in nature.
- Create a simulation and analysis pipeline development towards searching microlensing signals in the upcoming Roman data.

- Evaluation $\langle \bar{N} \rangle$ from the three-body capture and ejection crossections calculated so far
- More simulations on a larger variety of initial parameters, better analysis of the relation between the parameters that enable capture events and their occurrence in nature.
- Create a simulation and analysis pipeline development towards searching microlensing signals in the upcoming Roman data.

I also need to consider the three-body capture and ejection, and apply both capture mechanisms for a large number of systems. Then I will investigate the TESS data for microlensing events that might belong to a BH-MS system, and start preparing a pipeline to work with upcoming Roman data.

Part II: Galaxy-Scale Strong Lenses as a Probe of Dark Matter

Part II: Galaxy-Scale Strong Lenses as a Probe of Dark Matter

Another approach to the dark matter is that they might be hidden in the galaxy subhalos.

- In ΛCDM, gravity is the source that is responsible for the structure formation by hierarchical merging of smaller structures. Such structures are held in the gravitational potential well of the massive halo and referred to as sub-halos.

- In ΛCDM, gravity is the source that is responsible for the structure formation by hierarchical merging of smaller structures. Such structures are held in the gravitational potential well of the massive halo and referred to as sub-halos.

- In LambdaCDM, gravity is the source that is responsible for the structure formation by hierarchical merging of smaller structures. Such structures are held in the gravitational potential well of the massive halo and referred to as sub-halos

⇒ For ΛCDM, various studies by Navarro et al. utilizing N-body simulations led to a 'universal' density profile, known as **The Navarro–Frenk–White (NFW) profile** :

$$\frac{\rho(r)}{\rho_{crit}} = \frac{\delta_c}{\frac{r}{r_s}(1+\frac{r}{r_s})^2} \tag{14}$$

where r_s is the characteristic radius of the halo (scale radius), δ_c is the characteristic density and $\rho_{crit} = 3H^2/8\pi G$ is the critical density [18, 17].

⇒ For ΛCDM, various studies by Navarro et al. utilizing N-body simulations led to a 'universal' density profile, known as **The Navarro–Frenk–White (NFW) profile** :

$$\frac{\rho(r)}{\rho_{crit}} = \frac{\delta_c}{\frac{r}{r_s}(1+\frac{r}{r_s})^2} \tag{14}$$

where r_s is the characteristic radius of the halo (scale radius), δ_c is the characteristic density and $\rho_{crit} = 3H^2/8\pi G$ is the critical density [18, 17].

In literature, for the galaxy density profiles, the simulations indicate Navarro–Frenk–White model...

Subhalo Structure - Observations

⇒ The rotation curves inferred from the observations of the dark matter-dominated Low-Surface-Brightness(LSB) galaxies sides with the 'pseudo-isothermal' (PI) sphere profile,

$$\rho_{PI} = \frac{\rho_0}{1 + (\frac{r}{R_C})^2} \tag{15}$$

where R_C is the core radius of the halo [18, 2].

⇒ The rotation curves inferred from the observations of the dark matter-dominated Low-Surface-Brightness(LSB) galaxies sides with the 'pseudo-isothermal' (PI) sphere profile,

$$\rho_{PI} = \frac{\rho_0}{1 + (\frac{r}{R_C})^2} \tag{15}$$

where R_C is the core radius of the halo [18, 2].

While the observational data results in pseudo-isothermal' (PI) sphere profile.

Core-Cusp Problem

If $\rho \sim r^{\alpha}$, as r $\rightarrow 0$;

- The NFW density profile given by the simulations yields a slope with $\alpha = -1 \Leftrightarrow$ a *cusp*!
- The PI density profile inferred by the observed rotation curves indicates a constant density region with $\alpha = 0 \Leftrightarrow$ a *core*!

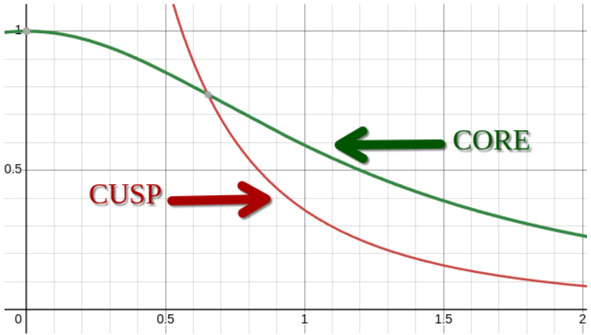

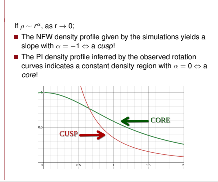

So, the simulations suggests a cusp towards the galactic center, but observations show that the density stays constant. This is known as the core-cusp problem.

Galaxy Scale Strong Lenses (GSSL)

$\longrightarrow$ *The small scale crisis in cosmology*

The discrepancy between the density profiles given by observations and simulations is known as the *core-cusp problem* [2].

- Possible solutions include warm dark matter (WDM) and self-interacting dark matter (SIDM) models as alternatives for the ΛCDM [8].
- SIDM predicts that the dark matter halos might undergo gravothermal collapse, resulting in a steep density profile formation and increased overall central halo density. In such a scenario, individual galaxies in clusters would act as strong lenses and produce arcseconds scale multiple images [25, 16].

The small scale crisis in cosmology
The discrepancy between the density profiles given by observations and simulations is known as the core-cusp problem [2].
Possible solutions include warm dark matter (WDM) and self-interacting dark matter (SIDM) models as alternatives for the ΛCDM [8].
SIDM predicts that the dark matter halos might undergo gravothermal collapse, resulting in a steep density profile formation and increased overall central halo density. In such a scenario, individual galaxies in clusters would act as strong lenses and produce arcseconds scale multiple images [25, 16].

Self interacting dark matter might be a solution. In this scenario, galaxies with high density central halos could act as strong lenses.

Galaxy Scale Strong Lenses (GSSL)

- Hence, GSSLs formed by massive elliptical galaxies and dwarf galaxies are expected to provide insights into the problem.
- Luckily, The Large Synoptic Survey Telescope (LSST) at the Rubin Observatory is expected to make an impactful contribution to the GSSL population from both galaxy types [22].
- At this part of my work, I will focus on the GSSL analysis in the upcoming LSST data, including possible effects of the contaminated exposures.

- Hence, GSSLs formed by massive elliptical galaxies and dwarf galaxies are expected to provide insights into the problem.
- Luckily, The Large Synoptic Survey Telescope (LSST) at the Rubin Observatory is expected to make an impactful contribution to the GSSL population from both galaxy types [22].
- At this part of my work, I will focus on the GSSL analysis in the upcoming LSST data, including possible effects of the contaminated exposures.

Therefore we turn to galaxy scale strong lenses. I will mainly focus on the analysis of the upcoming LSST data, including the contamination effects.

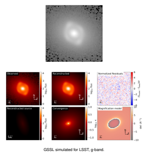

LSST Simulations on Lenstronomy

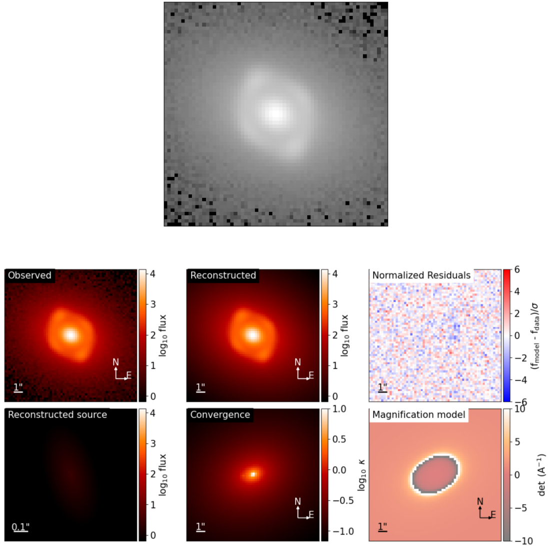

GSSL simulated for LSST, g-band.

- So far, I've been working on modeling and analysis of the mock LSST exposures for GSSLs that I simulated using LENSTRONOMY.

What's Next?

- Repeat the analysis procedure on the HSC data using LSST pipelines, determine R_C detection sensitivity with LSST.
- Include LSST observation simulations (ObSim) on the pipeline to prepare for detection and analysis of the GSSL on the upcoming LSST data.

- Repeat the analysis procedure on the HSC data using LSST pipelines, determine R_C detection sensitivity with LSST.
- Include LSST observation simulations (ObSim) on the pipeline to prepare for detection and analysis of the GSSL on the upcoming LSST data.

Soon, I will start working on the HSC data to determine core radius detection sensitivity. Then I will prepare a comprehensive pipeline for the detection and analysis of the GSSLs with LSST.

Thank you for listening!

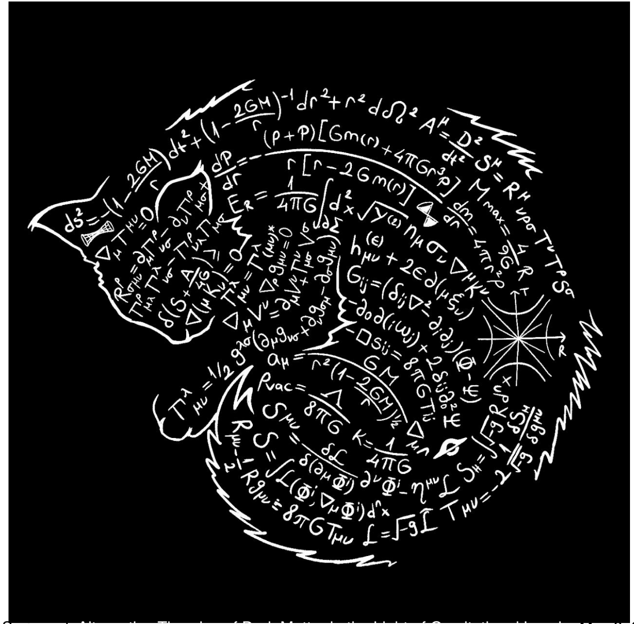

2025-05-09

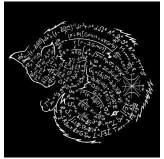

References I

[1] G. M. Beskin and A. V. Tuntsov. "Detection of compact objects by means of gravitational lensing in binary systems". en. In: *Astronomy & Astrophysics* 394.2 (Nov. 2002). Number: 2 Publisher: EDP Sciences, pp. 489–503. ISSN: 0004-6361, 1432-0746. DOI: 10.1051/0004-6361:20021150. URL: https://www.aanda.org/articles/aa/abs/2002/41/aa2132/aa2132.html (visited on 01/21/2025).

[2] W. J. G. de Blok. "The Core-Cusp Problem". en. In: *Advances in Astronomy* 2010.1 (2010). _eprint: https://onlinelibrary.wiley.com/doi/pdf/10.1155/2010/789293, p. 789293. ISSN: 1687-7977. DOI: 10.1155/2010/789293. URL: https://onlinelibrary.wiley.com/doi/abs/10.1155/2010/789293 (visited on 03/10/2025).

[3] B. J. Carr and James E. Lidsey. "Primordial black holes and generalized constraints on chaotic inflation". In: *Physical Review D* 48.2 (July 1993). Publisher: American Physical Society, pp. 543–553. DOI: 10.1103/PhysRevD.48.543. URL: https://link.aps.org/doi/10.1103/PhysRevD.48.543 (visited on 01/20/2025).

[4] Bernard Carr and Florian Kühnel. "Primordial black holes as dark matter candidates". en. In: *SciPost Physics Lecture Notes* (May 2022), p. 048. ISSN: 2590-1990. DOI: 10.21468/SciPostPhysLectNotes.48. URL: https://scipost.org/10.21468/SciPostPhysLectNotes.48 (visited on 01/20/2025).

[5] Bernard Carr and Florian Kühnel. "Primordial Black Holes as Dark Matter: Recent Developments". In: *Annual Review of Nuclear and Particle Science* 70.1 (Oct. 2020), pp. 355–394. ISSN: 1545-4134. DOI: 10.1146/annurev-nucl-050520-125911. URL: http://dx.doi.org/10.1146/annurev-nucl-050520-125911.

[6] Bernard Carr et al. "Constraints on primordial black holes". In: *Reports on Progress in Physics* 84 (Nov. 2021). Publisher: IOP ADS Bibcode: 2021RPPh...84k6902C, p. 116902. ISSN: 0034-4885. DOI: 10.1088/1361-6633/ac1e31. URL: https://ui.adsabs.harvard.edu/abs/2021RPPh...84k6902C (visited on 02/24/2025).

References II

[7] Sean M. Carroll. *Spacetime and Geometry: An Introduction to General Relativity*. en. ISBN: 9781108770385 Publisher: Cambridge University Press. Aug. 2019. DOI: 10.1017/9781108770385. URL: https://www.cambridge.org/highereducation/books/spacetime-and-geometry/38EDABF9E2BADCE6FBCF2B22DC12BFFE (visited on 04/22/2025).

[8] Oliver D. Elbert et al. "Core formation in dwarf haloes with self-interacting dark matter: no fine-tuning necessary". In: *Monthly Notices of the Royal Astronomical Society* 453.1 (Oct. 2015), pp. 29–37. ISSN: 0035-8711. DOI: 10.1093/mnras/stv1470. URL: https://doi.org/10.1093/mnras/stv1470 (visited on 03/10/2025).

[9] Stephen Hawking. "Gravitationally Collapsed Objects of Very Low Mass". In: *Monthly Notices of the Royal Astronomical Society* 152.1 (Apr. 1971), pp. 75–78. ISSN: 0035-8711. DOI: 10.1093/mnras/152.1.75. eprint: https://academic.oup.com/mnras/article-pdf/152/1/75/9360899/mnras152-0075.pdf. URL: https://doi.org/10.1093/mnras/152.1.75.

[10] P. Ivanov, P. Naselsky, and I. Novikov. "Inflation and primordial black holes as dark matter". In: *Physical Review D* 50.12 (Dec. 1994). Publisher: American Physical Society, pp. 7173–7178. DOI: 10.1103/PhysRevD.50.7173. URL: https://link.aps.org/doi/10.1103/PhysRevD.50.7173 (visited on 01/20/2025).

[11] Benjamin V. Lehmann, Stefano Profumo, and Jackson Yant. "The maximal-density mass function for primordial black hole dark matter". en. In: *Journal of Cosmology and Astroparticle Physics* 2018.04 (Apr. 2018), p. 007. ISSN: 1475-7516. DOI: 10.1088/1475-7516/2018/04/007. URL: https://dx.doi.org/10.1088/1475-7516/2018/04/007 (visited on 02/24/2025).

[12] Benjamin V. Lehmann et al. "Capture of primordial black holes in extrasolar systems". en. In: *Journal of Cosmology and Astroparticle Physics* 2022.08 (Aug. 2022), p. 079. ISSN: 1475-7516. DOI: 10.1088/1475-7516/2022/08/079. URL: https://iopscience.iop.org/article/10.1088/1475-7516/2022/08/079 (visited on 12/30/2024).

References III

[13] A. Maeder. "Light Curves of the Gravitational Lens-like Action for Binaries with Degenerate Stars". In: *Astronomy and Astrophysics* 26 (July 1973). ADS Bibcode: 1973A&A....26..215M, p. 215. ISSN: 0004-6361. URL: https://ui.adsabs.harvard.edu/abs/1973A&A....26..215M (visited on 01/20/2025).

[14] Kento Masuda and Kenta Hotokezaka. "Prospects of Finding Detached Black Hole-Star Binaries with TESS". In: *The Astrophysical Journal* 883.2 (Oct. 2019). arXiv:1808.10856 [astro-ph], p. 169. ISSN: 0004-637X, 1538-4357. DOI: 10.3847/1538-4357/ab3a4f. URL: http://arxiv.org/abs/1808.10856 (visited on 01/18/2025).

[15] Kento Masuda and Kenta Hotokezaka. "Prospects of Finding Detached Black Hole-Star Binaries with TESS". In: *The Astrophysical Journal* 883.2 (Oct. 2019). arXiv:1808.10856 [astro-ph], p. 169. ISSN: 0004-637X, 1538-4357. DOI: 10.3847/1538-4357/ab3a4f. URL: http://arxiv.org/abs/1808.10856 (visited on 01/18/2025).

[16] P. Natarajan et al. "Strong Lensing by Galaxy Clusters". en. In: *Space Science Reviews* 220.2 (Feb. 2024), p. 19. ISSN: 1572-9672. DOI: 10.1007/s11214-024-01051-8. URL: https://doi.org/10.1007/s11214-024-01051-8 (visited on 03/10/2025).

[17] Julio F. Navarro, Carlos S. Frenk, and Simon D. M. White. "A Universal Density Profile from Hierarchical Clustering". en. In: *The Astrophysical Journal* 490.2 (Dec. 1997). Publisher: IOP Publishing, p. 493. ISSN: 0004-637X. DOI: 10.1086/304888. URL: https://iopscience.iop.org/article/10.1086/304888/meta (visited on 03/20/2025).

[18] Julio F. Navarro, Carlos S. Frenk, and Simon D. M. White. "The Structure of Cold Dark Matter Halos". In: *The Astrophysical Journal* 462 (May 1996). Publisher: IOP ADS Bibcode: 1996ApJ...462..563N, p. 563. ISSN: 0004-637X. DOI: 10.1086/177173. URL: https://ui.adsabs.harvard.edu/abs/1996ApJ...462..563N (visited on 03/20/2025).

[19] S. Rahvar, A. Mehrabi, and M. Dominik. "Compact object detection in self-lensing binary systems with a main-sequence star". In: *Monthly Notices of the Royal Astronomical Society* 410.2 (Jan. 2011), pp. 912–918. ISSN: 0035-8711. DOI: 10.1111/j.1365-2966.2010.17490.x. URL: https://doi.org/10.1111/j.1365-2966.2010.17490.x (visited on 01/20/2025).

2025-05-09

References IV

[20] Jeff Riley et al. "Rapid Stellar and Binary Population Synthesis with COMPAS". In: *The Astrophysical Journal Supplement Series* 258 (Feb. 2022). Publisher: IOP ADS Bibcode: 2022ApJS..258...34R, p. 34. ISSN: 0067-0049. DOI: 10.3847/1538-4365/ac416c. URL: https://ui.adsabs.harvard.edu/abs/2022ApJS..258...34R (visited on 02/04/2025).

[21] Misao Sasaki et al. "Primordial black holes—perspectives in gravitational wave astronomy". In: *Classical and Quantum Gravity* 35.6 (Feb. 2018), p. 063001. DOI: 10.1088/1361-6382/aaa7b4. URL: https://dx.doi.org/10.1088/1361-6382/aaa7b4.

[22] Anowar J. Shajib et al. *Strong gravitational lenses from the Vera C. Rubin Observatory*. arXiv:2406.08919 [astro-ph]. Feb. 2025. DOI: 10.48550/arXiv.2406.08919. URL: http://arxiv.org/abs/2406.08919 (visited on 03/10/2025).

[23] M. Turner. "Gravitational radiation from point-masses in unbound orbits - Newtonian results". en. In: *The Astrophysical Journal* 216 (Sept. 1977), p. 610. ISSN: 0004-637X, 1538-4357. DOI: 10.1086/155501. URL: http://adsabs.harvard.edu/doi/10.1086/155501 (visited on 04/23/2025).

[24] Pablo Villanueva-Domingo, Olga Mena, and Sergio Palomares-Ruiz. "A Brief Review on Primordial Black Holes as Dark Matter". en. In: *Frontiers in Astronomy and Space Sciences* 8 (May 2021), p. 681084. ISSN: 2296-987X. DOI: 10.3389/fspas.2021.681084. URL: https://www.frontiersin.org/articles/10.3389/fspas.2021.681084/full (visited on 12/30/2024).

[25] Daneng Yang and Hai-Bo Yu. "Self-interacting dark matter and small-scale gravitational lenses in galaxy clusters". In: *Physical Review D* 104.10 (Nov. 2021). Publisher: American Physical Society, p. 103031. DOI: 10.1103/PhysRevD.104.103031. URL: https://link.aps.org/doi/10.1103/PhysRevD.104.103031 (visited on 03/20/2025).

[26] Ya. B. Zel'dovich and I. D. Novikov. "The Hypothesis of Cores Retarded during Expansion and the Hot Cosmological Model". In: 43 (Jan. 1966), p. 758.

2025-05-09

References V

[27] Saiyang Zhang, Volker Bromm, and Boyuan Liu. "How Do Primordial Black Holes Change the Halo Mass Function and Structure?" en. In: *The Astrophysical Journal* 975.1 (Oct. 2024). Publisher: The American Astronomical Society, p. 139. ISSN: 0004-637X. DOI: 10.3847/1538-4357/ad7b0d. URL: https://dx.doi.org/10.3847/1538-4357/ad7b0d (visited on 02/24/2025).

[27] Saiyang Zhang, Volker Bromm, and Boyuan Liu. "How Do Primordial Black Holes Change the Halo Mass Function and Structure?" en. In: The Astrophysical Journal 975.1 (Oct. 2024). Publisher: The American Astronomical Society, p. 139. ISSN: 0004-637X. DOI: 10.3847/1538-4357/ad7b0d. URL: https://dx.doi.org/10.3847/1538-4357/ad7b0d (visited on 02/24/2025).

What are primordial black holes?

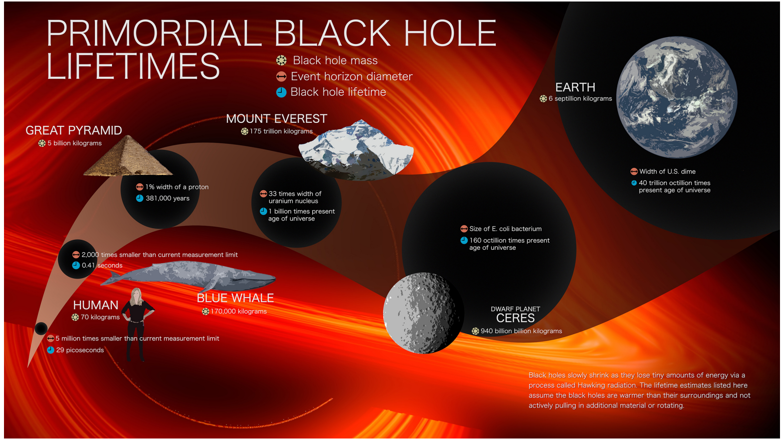

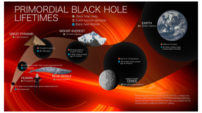

- It's been 50 years since they were first proposed, but we have not confirmed one yet.

What are primordial black holes?

- Primordial black holes (PBHs) are hypothetical objects that could have formed as highly over-dense regions collapse gravitationally in the early universe, by mechanisms such as adiabatic quantum fluctuations appearing during inflation [3, 10], collapse from density fluctuations and various collapse scenarios including domain walls, cosmic loops, bubble collisions [4].
- They have non-stellar origins [21].
- First suggested in [26], and also independently in [9], they have been a source of attention for almost 50 years due to their extraordinary properties such as constituting primordial non-baryonic matter from the radiation-dominated era [24, 5]

- Primordial black holes (PBHs) are hypothetical objects that could have formed as highly over-dense regions collapse gravitationally in the early universe, by mechanisms such as adiabatic quantum fluctuations appearing during inflation [3, 10], collapse from density fluctuations and various collapse scenarios including domain walls, cosmic loops, bubble collisions [4].
- They have non-stellar origins [21].
- First suggested in [26], and also independently in [9], they have been a source of attention for almost 50 years due to their extraordinary properties such as constituting primordial non-baryonic matter from the radiation-dominated era [24, 5]

Mass Models

- They can be small enough to get affected by the Hawking radiation, smaller than 10^{15}g.[**kuhler**]
- Therefore it is wiser to inspect primordial black holes (PBHs) more massive than that.
- For PHBs to be accounted for the cold dark matter, they should be in one of these mass windows [**kuhler**]:
  $\longrightarrow$ the asteroid mass range($10^{16} - 10^{17}$g)
  $\longrightarrow$ the sublunar mass range ($10^{20} - 10^{26}$g)
  $\longrightarrow$ the intermediate mass range (10-10^3 M_{sun})
- Even if they fall into one of these windows, they may not provide *all* dark matter [**kuhler**].

DISCLAIMER

They can be small enough to get affected by the Hawking radiation, smaller than 10^{15}g.[**kuhler**]
Therefore it is wiser to inspect primordial black holes (PBHs) more massive than that.
For PHBs to be accounted for the cold dark matter, they should be in one of these mass windows [**kuhler**]:
$\longrightarrow$ the asteroid mass range($10^{16} - 10^{17}$g)
$\longrightarrow$ the sublunar mass range ($10^{20} - 10^{26}$g)
$\longrightarrow$ the intermediate mass range (10-10^3 M_{sun})
Even if they fall into one of these windows, they may not provide *all* dark matter [**kuhler**].
DISCLAIMER

From Carr et al., 2021 [6]

other cosmological conundra. In particular, many authors have discussed the possibility that PBHs could provide the dark matter [22, 562]. In this context, Fig. 10 might suggest that the asteroid range $10^{17}\,\mathrm{g} < M < 10^{23}\,\mathrm{g}$ between the EGB and HSC microlensing limits is most plausible. However, the intermediate range $10\,M_\odot < M < 10^2\,M_\odot$ between the LMC microlensing and wide binary limits is still favored by some theorists, even though this appears to violate other constraints, because PBHs may naturally form in this range. In principle, Fig. 10 suggests that a lot of dark matter could reside in "stupendously large black holes" in the range $10^{14}\,M_\odot < M < 10^{17}\,M_\odot$, although the lack of constraints there probably just reflects the fact that little attention has been paid to this possibility and obviously such SLABs could not provide dark matter inside galactic halos [426]. A final possibility is the Planck-mass relics of Hawking evaporation in the range around $M \sim 10^{-5}\,\mathrm{g}$, although this is probably untestable unless the relics are electrically charged [138].

From Carr et al., 2021 [6]

are lots of however and although everywhere...

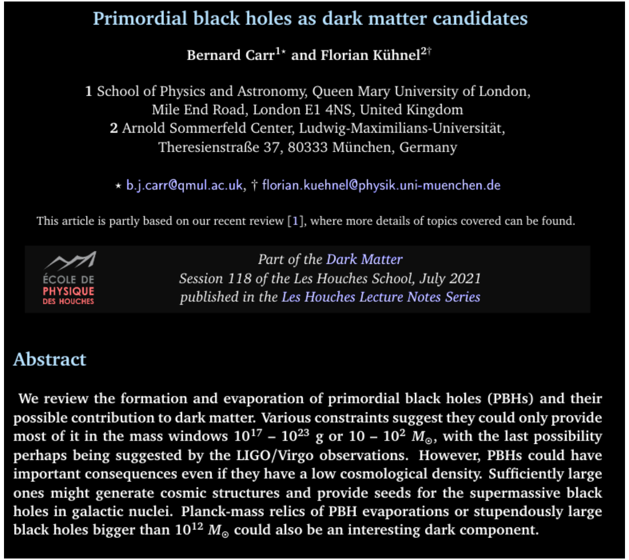

Primordial black holes as dark matter candidates

Bernard Carr[1*] and Florian Kühnel[2†]

1 School of Physics and Astronomy, Queen Mary University of London,
Mile End Road, London E1 4NS, United Kingdom
2 Arnold Sommerfeld Center, Ludwig-Maximilians-Universität,
Theresienstraße 37, 80333 München, Germany

⋆ b.j.carr@qmul.ac.uk, † florian.kuehnel@physik.uni-muenchen.de

This article is partly based on our recent review [1], where more details of topics covered can be found.

ÉCOLE DE PHYSIQUE DES HOUCHES

Part of the Dark Matter
Session 118 of the Les Houches School, July 2021
published in the Les Houches Lecture Notes Series

Abstract

We review the formation and evaporation of primordial black holes (PBHs) and their possible contribution to dark matter. Various constraints suggest they could only provide most of it in the mass windows $10^{17} - 10^{23}$ g or $10 - 10^{2}\ M_{\odot}$, with the last possibility perhaps being suggested by the LIGO/Virgo observations. However, PBHs could have important consequences even if they have a low cosmological density. Sufficiently large ones might generate cosmic structures and provide seeds for the supermassive black holes in galactic nuclei. Planck-mass relics of PBH evaporations or stupendously large black holes bigger than $10^{12}\ M_{\odot}$ could also be an interesting dark component.

Alternative Theories of Dark Matter in the Light of Gravitational Lensing
Appendix
Mass Models

2025-05-09

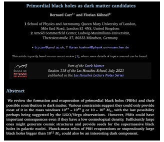

studies arguing about it, so many uncertainties. So I decided to be open-minded for the mass ranges that I will be looking for this project other than the ones naturally emerge by the observational limits

Why Black Hole - Main Sequence Star (BH-MS) Binaries?

- Primordial black holes in binary systems are detectable by their impact on the binary star light curves as a result of self-lensing.
- Initial work on compact object (CO) self-microlensing detectability considered MS star companions as unfavorable candidates compared to white dwarfs, since the source radius and the lens effect are inversely proportional [1].
- However, having more achievable photometry on brighter targets and a higher population to be monitored, Rahvar et al. [19] showed that MS stars are not less favorable targets than other CO.

- Primordial black holes in binary systems are detectable by their impact on the binary star light curves as a result of self-lensing.
- Initial work on compact object (CO) self-microlensing detectability considered MS star companions as unfavorable candidates compared to white dwarfs, since the source radius and the lens effect are inversely proportional [1].
- However, having more achievable photometry on brighter targets and a higher population to be monitored, Rahvar et al. [19] showed that MS stars are not less favorable targets than other CO.

-lensing in binary systems occurs when the compact object gravitationally deflects the light from the star as it transits

Maeder [13].

So their relatively higher brightness magnitudes is why we study MS stars as PBH companions in this work.

Stellar Evolution Binary System Distributions via COMPAS

- I use the rapid stellar and binary population synthesis tool COMPAS to simulate parameter distribution and occurrence of BH-MS systems in nature [20].

I use the rapid stellar and binary population synthesis tool COMPAS to simulate parameter distribution and occurrence of BH-MS systems in nature [20].

work focuses on particular input parameters such as the initial masses of the primary and secondary stars, the initial semi-major axis, and the initial mass function as a parameter for the population characteristics. All the remaining parameters required for the simulation to run are taken as the default values. Both primary and secondary stars ('Primary' refers to the companion with the higher mass in the binary while 'secondary' is the lower mass companion) in every binary start their evolution as MS stars with masses sampled from Kroupa Initial Mass Function. Characteristic events of the stellar evolution such as common envelope (CE) formation and mass transfer (MT) events can be tracked for the simulated binaries during their lifetime. Preliminary simulations show that about 58% of the binaries undergo MT events that have a substantial impact on the binary system not only by altering the mass distribution but also by initiating the stellar-type transformations of the companions. Binaries may have multiple MT events that enable their evolution into any stellar type on Table 2 in [20]. Depending on the initial parameters and MT events, binaries can undergo supernovae, form double compact objects (DCO), unbound binaries, or mergers.

Binary Occurrences

We take the mean occurrence plots on Masuda & Hotokezaka's work [14] as a basis to reproduce them using COMPAS results.

Prospects of Finding Detached Black Hole–Star Binaries with *TESS*

Kento Masuda[1] and Kenta Hotokezaka
Department of Astrophysical Sciences, Princeton University, Princeton, NJ 08544, USA; kmasuda@astro.princeton.edu
Received 2018 August 31; revised 2019 August 1; accepted 2019 August 8; published 2019 October 1

Abstract

We discuss prospects of identifying and characterizing black hole (BH) companions to normal stars on tight but detached orbits, using photometric data from the *Transiting Exoplanet Survey Satellite* (*TESS*). We focus on the following two periodic signals from the visible stellar component: (i) in-eclipse brightening of the star due to gravitational microlensing by the BH (self-lensing), and (ii) a combination of ellipsoidal variations due to tidal distortion of the star and relativistic beaming due to its orbital motion (phase-curve variation). We evaluate the detectability of each signal in the light curves of stars in the *TESS* input catalog, based on a pre-launch noise model of *TESS* photometry as well as the actual light curves of spotted stars from the prime *Kepler* mission to gauge the potential impact of stellar activity arising from the tidally spun-up stellar components. We estimate that the self-lensing and phase-curve signals from BH companions, if they exist, will be detectable in the light curves of effectively $\mathcal{O}(10^5)$ and $\mathcal{O}(10^6)$ low-mass stars, respectively, taking into account orbital inclination dependence of the signals. These numbers could be large enough to actually detect signals from BHs: simple population models predict some 10 and 100 detectable BHs among these "searchable" stars; although, the latter may be associated with a comparable number of false positives due to stellar variabilities, and additional vetting with radial velocity measurements would be essential. Thus, the *TESS* data could serve as a resource to study nearby BHs with stellar companions on shorter-period orbits than will potentially be probed with *Gaia*.

Key words: stars: black holes – stars: neutron – techniques: photometric – white dwarfs

We take the mean occurrence plots on Masuda & Hotokezaka's work [14] as a basis to reproduce them using COMPAS results.

Residuals

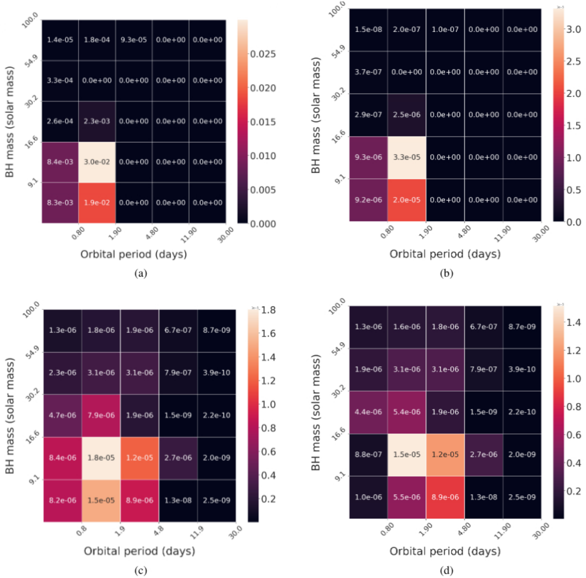

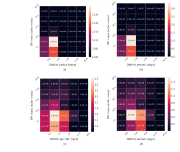

(a) Occurrence rate distribution over black hole mass and orbital period for BH-MS binaries after their last MT event for $T < 30$ (days), (b) after applying searchability index of 0.0011, (c) occurrence rate distribution over black hole mass - orbital period for binaries searchable via self lensing adapted Figure 4b by Masuda and Hotokezaka [14], (d) residuals of b & c. Stellar evolution simulation by COMPAS processed by LUXETENEBRAE.

⇒In Masuda & Hotokezaka [15], the 'searchability' constraint includes various criteria such as recovery rate as a function of the signal-to-noise ratio C_{rec} and the eclipse probability R_{star}/a

$$N_{eff} = \frac{R_{star}}{a} C_{rec}(\sqrt{n}\frac{S_{self-lensing}}{\sigma_{30min}}) \tag{16}$$

while the values compared above only include the criteria of edge-on configuration for the binaries, given by $cos_i \leq cos(89.9) \approx cos(\pi/2) = 0$

$$cos_i \leq cos(89.9) \approx cos(\pi/2) = 0 \tag{17}$$

which yields a *searchability index* of ≈ 0.0011.

⇒In Masuda & Hotokezaka [15], the 'searchability' constraint includes various criteria such as recovery rate as a function of the signal-to-noise ratio C_{rec} and the eclipse probability R_{star}/a

$$N_{eff} = \frac{R_{star}}{a} C_{rec}(\sqrt{n}\frac{S_{self-lensing}}{\sigma_{30min}}) \tag{16}$$

while the values compared above only include the criteria of edge-on configuration for the binaries, given by $cos_i \leq cos(89.9) \approx cos(\pi/2) = 0$

$$cos_i \leq cos(89.9) \approx cos(\pi/2) = 0 \tag{17}$$

which yields a *searchability index* of ≈ 0.0011.

main cause of the current residual values is the duality of the searchability criteria. I will evaluate the additional constraints and minimize the residuals to confirm that the occurrence rates from COMPAS simulation are reasonable and in line with the occurrence rates expected from TESS by Masuda and Hotokezaka [14]. Then, in the first part of this task, I will search for microlensing events in TESS data with predicted mass and semimajor axis parameters to compare with the COMPAS results. A discrepancy between the predicted and observed populations where observed abundancy is higher or a discrepancy of the peak semimajor axis might indicate BH-MS systems formed by capture.

Statistics Summary

Table 1: Updated quantities from the simulation log file.

Quantity	Pre-MT	Post-MT	Post Last MT
Number of systems	29,000,000	-	-
Number of systems forming MT (via SP STATUS)	17,029,983	-	-
Number of primary mass BHs	2,207,804	2,671,970	-
Number of secondary mass BHs	513,929	2,132	-
Number of unbound binaries	1,851,730	-	-
Number of double compact objects	863	-	-
Number of mergers	0	-	-
Number of BH-NS binaries	0	3,533	-
Number of NS-BH binaries	0	269	-
Number of BH-MS binaries	1,398,490	1,441,991	29,740
Number of MS-BH binaries	0	0	0
Number of systems with semimajor axis < 3.0 AU BH-MS binaries	1,398,149	1,441,991	29,740
Number of systems with semimajor axis < 3.0 AU MS-BH binaries	0	0	-
Number of systems with orbital period < 70 days BH-MS binaries	1,397,834	1,441,624	29,660
Number of systems with orbital period < 70 days MS-BH binaries	0	0	0
Number of systems with orbital period < 30 days BH-MS binaries	-	1,440,658	29,384
Number of systems with orbital period < 30 days MS-BH binaries	-	0	0
Number of systems with semimajor axis < 0.4 AU BH-MS binaries	-	1,440,600	29,380
Number of systems with semimajor axis < 0.4 AU MS-BH binaries	-	0	0
Number of systems with orbital inclination (COSI) < 89.99° BH-MS binaries	1,539	1,656	38
Number of systems with orbital inclination (COSI) < 89.99° MS-BH binaries	0	0	0

results show that among 58.72% of the binaries are undergoing MT events about 0.17% of these systems end up in BH-MS binaries. 99.73% of these BH-MS binaries have orbital periods shorter than 70 days within the observational limits of the Roman. For total population, this corresponds to 0.10%.

Capture crossection from 3-body encounters

$$\widetilde{\sigma}_{\rm ej} = \pi \left(\frac{2M_B r_{AB}}{5M_A}\right)^2 \left[-1 - \left(\frac{v_B^2 r_{AB} - 2\mu_A}{2v_B^2 r_{AB} + \mu_A}\right)^2 - \frac{v_B^2 r_{AB} + 2\mu_A}{v_B\sqrt{\mu_A r_{AB}/2}} \arctan\left(\frac{2v_B\sqrt{2\mu_A r_{AB}}}{\mu_A - 2v_B^2 r_{AB}}\right)\right. \tag{18}$$

$$\widetilde{\sigma}_{\rm cap} \equiv \pi \left(\frac{\mu_B}{v_1^2 - v_{\rm esc}^2}\right)^2 \left[-1 - \left(\frac{v_{\rm esc}^2 - v_B^2}{v_1^2 - v_B^2}\right)^2 + \frac{v_{\rm esc}^2 + v_B^2}{v_1 v_B} \arctan\left(\frac{2v_1 v_B}{v_1^2 + v_B^2}\right)\right. . \tag{19}$$

Side Quest: Investigating Streak Contamination

As an explanatory case, we choose to work with Starlink constellations
10 Days Starlink Positions
↪ Altitude of the of 6412 Starlink satellites with 6-second iteration intervals throughout the night observed from the Rubin Observatory in Cerro Pachón, Chile. The color scale demonstrates the azimuth of the satellite in the sky.

As an explanatory case, we choose to work with Starlink constellations
10 Days Starlink Positions
↪ Altitude of the of 6412 Starlink satellites with 6-second iteration intervals throughout the night observed from the Rubin Observatory in Cerro Pachón, Chile. The color scale demonstrates the azimuth of the satellite in the sky.

Side Quest: Investigating Streak Contamination

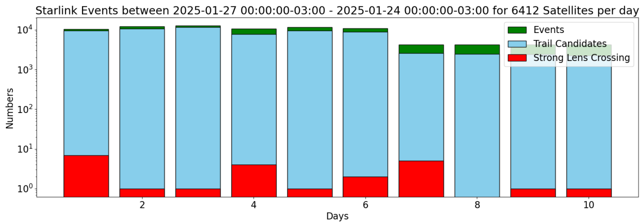

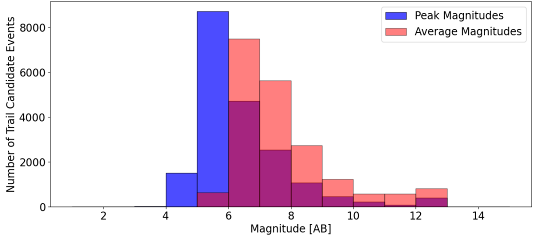

The peak magnitudes of the satellites during each trail event window and the average of these peak magnitudes for each trail event window in arcseconds.

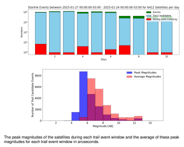

: all starlink events above 30 degrees for each satellite within 24h.

Blue: trail candidates, green conditions plus during outside the day time and reflecting sunlight

Side Quest: Investigating Streak Contamination

The LSST survey is challenged by the increasing number of Sun-reflecting artificial satellites. Here we focus on the Low Earth Orbit (LEO) satellites, which are brighter due to their lower altitudes and contributing as a larger population.

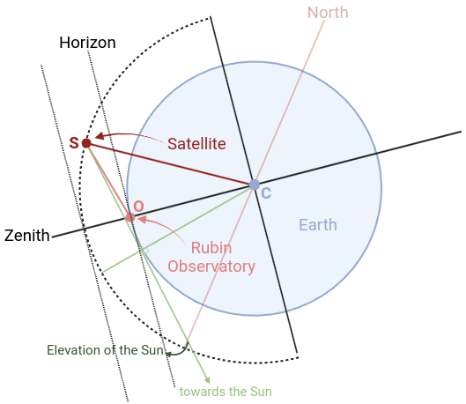

The LSST survey is challenged by the increasing number of Sun-reflecting artificial satellites. Here we focus on the Low Earth Orbit (LEO) satellites, which are brighter due to their lower altitudes and contributing as a larger population.